Effect of Anisotropy on Springback of Integrated Circuit Leadframes

K.C. Chan and S.H. Wang

(Submitted 11 March 1998; in revised form 25 January 1999)

In order to meet the stringent requirements for high lead count packages, a thorough understanding of springback behavior becomes essential in the forming of integrated circuit leadframes. Plastic anisotropy of leadframe materials is known to be one of the key factors affecting springback. However, insufficient theoretical work has been done in the past to study the effect of plastic anisotropy on springback in integrated circuit leadframe forming. In this paper, a new plane stress bending model, taking account of plastic anisotropy, has been proposed to predict the deformation behavior and springback of narrow strips. Comparisons between theoretical predictions and experimental results have been made. It is shown that the results predicted by the anisotropic model are in better agreement with the experimental observations than those given by the isotropic plane stress model. These findings are significant because they provide useful guidelines for tool designers.

Keywords anisotropy, computer analysis, microelectronics, plane stress

1. Introduction

In the design of forming dies for integrated circuit (IC) leadframes, tool designers must consider the springback problem in order to ensure that the final bend angle and the final radius conform to the specifications. Higher lead counts and smaller packages impose even more stringent demands on the forming quality and the precision of the tooling. For a better understanding of the springback behavior of IC leadframes, the authors and their coworkers have performed a series of experiments to investigate the deformation behavior and springback of IC leadframes using a special cantilever-type forming jig (Ref 1, 2), and a strain-hardening plane stress bending model has been proposed. In their experiments, the amount of springback has been found to increase with increasing die radius, die angle, and die gap. Significant anisotropy in the sheet materials has shown to result in different springback behaviors for different sheet orientations. The springback of the leadframe along the rolling direction has been found to be greater than that transverse to the rolling direction. Although much improvement has been achieved by using the plane stress model compared to the results based on the plane strain model, the effect of anisotropy has not been considered in the previous investigation.

It is well known that metal sheets manufactured by a combination of rolling and heat treatment exhibit plastic anisotropy. There are two sources of plastic anisotropy in metal sheets. They are (a) crystallographic anisotropy arising from preferred orientations or textures and (b) microstructural anisotropy caused by variations in grain size and shape, inclusion stringers, nonuniform distribution of phases, etc. In published literature, there has been a considerable amount of theoretical works predicting anisotropy from preferred orientations (Ref 3, 4). The effect of anisotropy on deformation behavior of metal sheets in various conventional forming processes has also been extensively investigated in the past decades (Ref 5, 6). However relatively little work has been done to study the effect of anisotropy on the springback of IC leadframes. Investigations in this area are therefore highly significant. In the present study, a new plane stress bending model taking into account the effect of plastic anisotropy is proposed to predict the deformation behavior and springback of narrow strips. The amount of spring-

K.C. Chan and **S.H. Wang,** Department of Manufacturing Engineering, The Hong Kong Polytechnic University, Hung Hom, Kowloon, Hong Kong. Contact e-mail: mfkechan@inet.polyu.edu.hk.

Nomenclature

k	Strength coefficient
l_o	Original length
n	Strain hardening exponent
P	Strain ratio in y-direction tension test
r	Arbitrary radius
r_i	Internal radius
r_u	Initial fiber radius
r'_u	Final unstretched fiber radius
r_y	External radius
R	Strain ratio in x-direction tension test
t_o	Original thickness
w	Arbitrary width
w_o	Original width
Greek symbols	
$\bar{\varepsilon}$	Effective strain
ε_x	Circumference strain
ε_y	Transverse strain
ε_z	Radial strain
θ	Initial bend angle
θ'	Final strip angle
$\bar{\sigma}$	Effective stress
σ_s	Initial yield stress
σ_x	Circumference stress
σ_y	Transverse stress
σ_z	Radial stress

back of one typical leadframe material is estimated, and the results are compared with published experimental findings.

2. The Model

In the present theoretical model, a narrow metal strip deformed under pure bending is considered. The material is anisotropic, and a plane stress state is assumed. The Bauschinger effect on load reversal is assumed to be negligible. Figure 1 illustrates the geometry of a bent strip, which is subjected to pure bending in its plane.

The force equilibrium equation for plane stress bending is expressed by:

$$\frac{d\sigma_z}{dr} = \frac{\sigma_x - \sigma_z}{r} - \frac{\sigma_z}{w}\frac{dw}{dr} \qquad \text{(Eq 1)}$$

In this model, Hill's anisotropic yield criterion is used (Ref 7). If the principal stress axes are chosen to be coincident with the axes of anisotropy, the yield criterion under plane stress condition is expressed as:

$$R\sigma_z^2 + RP\sigma_x^2 + P(\sigma_z - \sigma_x)^2 = \frac{2(P + R + PR)}{3}\bar{\sigma}^2 \qquad \text{(Eq 2)}$$

where:

$$R = R_0 = \frac{d\varepsilon_y}{d\varepsilon_z} \qquad \text{(Eq 3)}$$

$$P = R_{90} = \frac{d\varepsilon_x}{d\varepsilon_z} \qquad \text{(Eq 4)}$$

The circumferential true strain and the transverse true strain are given by:

$$\varepsilon_x = \ln\frac{r}{r_u} \qquad \text{(Eq 5)}$$

$$\varepsilon_y = \ln\frac{w}{w_o} \qquad \text{(Eq 6)}$$

Using Hill's yield criterion and following the deformation theory of plasticity, the stress-strain relations can be written as:

$$\varepsilon_y = -\frac{PR\sigma_x + R\sigma_z}{P(1+R)\sigma_x - P\sigma_z}\cdot\varepsilon_x \qquad \text{(Eq 7)}$$

$$\varepsilon_z = -\frac{P\sigma_x - (P+R)\sigma_z}{P(1+R)\sigma_x - P\sigma_z}\cdot\varepsilon_x \qquad \text{(Eq 8)}$$

The equivalent strain is:

$$\bar{\varepsilon} = \sqrt{\frac{2(P+R+PR)}{3PR(1+P+R)^2}\cdot\left[P(\varepsilon_y - R\varepsilon_z)^2 + R(P\varepsilon_z - \varepsilon_x)^2 + (R\varepsilon_x - P\varepsilon_y)^2\right]} \qquad \text{(Eq 9)}$$

The relationship between the equivalent strain and the circumferential strain thus becomes:

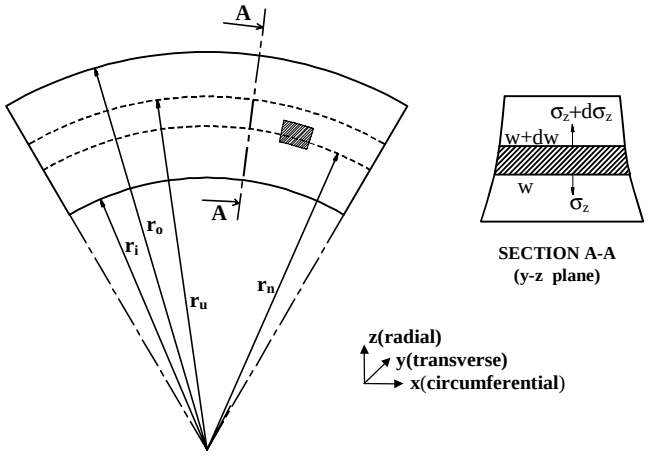

Fig. 1 Geometry of a bent narrow strip

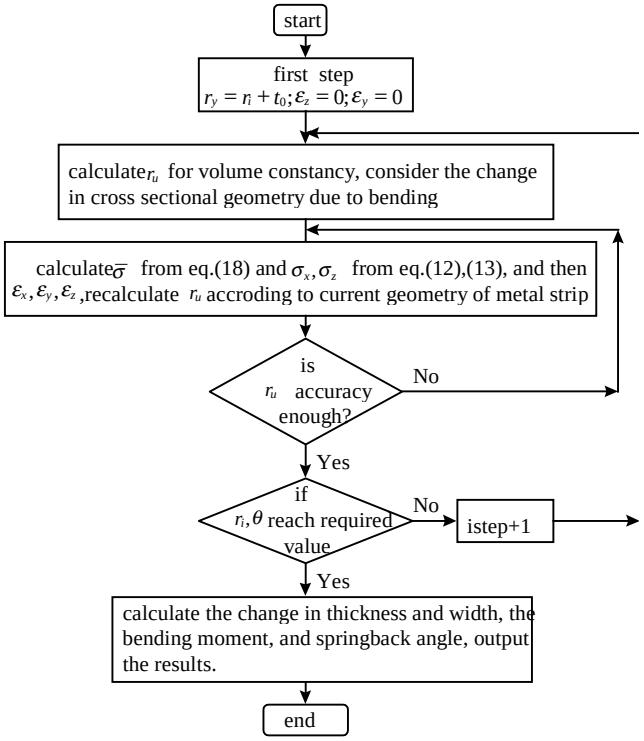

Fig. 2 Computational scheme of the model

$$\bar{\varepsilon} = -\frac{2}{3} \cdot \frac{(P + R + PR)\bar{\sigma}}{P(1 + R)\sigma_x - P\sigma_z} \cdot \varepsilon_x \qquad \text{(Eq 10)}$$

Assuming that the materials obey the isotropic strain hardening rule, Ludwik's empirical law is employed:

$$\bar{\sigma} = \sigma_s + k\bar{\varepsilon}^n \qquad \text{(Eq 11)}$$

From Eq 2, 10, and 11, the circumferential stress, σ_x, and the radial stress, σ_z, are then given by:

$$\sigma_x = \frac{2(P + R + PR)}{3P(1 + R)} \cdot \frac{\bar{\sigma} \ln \frac{r}{r_u}}{\left(\frac{\bar{\sigma} - \sigma_s}{k}\right)^{1/n}} + \frac{\sigma_z}{1 + R} \qquad \text{(Eq 12)}$$

$$\sigma_z = -\left[\frac{2(1 + R)(P + R + PR)}{3R(1 + P + R)} \cdot \bar{\sigma}^2 - \frac{4(P + R + PR)^2}{9PR(1 + P + R)} \cdot \frac{\bar{\sigma}^2 \left(\ln \frac{r}{r_u}\right)^2}{\left(\frac{\bar{\sigma} - \sigma_s}{k}\right)^{2/n}} \right]^{1/2} \qquad \text{(Eq 13)}$$

The stress equilibrium Eq 1 now becomes:

$$\frac{d\sigma_z}{dr} = \frac{\sigma_x - \sigma_z}{r} - \sigma_z \frac{d\varepsilon_y}{dr} \qquad \text{(Eq 14)}$$

The differentiation of Eq 7 with respect to r gives:

$$\frac{d\varepsilon_y}{dr} = -\frac{PR(1 + P + R)\left[\sigma_x \cdot \frac{d\sigma_z}{dr} - \sigma_z \cdot \frac{d\sigma_x}{dr}\right]}{[P(1 + R)\sigma_x - P\sigma_z]^2} \cdot \ln \frac{r}{r_u} - \frac{1}{r} \cdot \frac{PR\sigma_x + R\sigma_z}{P(1 + R)\sigma_x - P\sigma_z} \qquad \text{(Eq 15)}$$

Also by differentiating Eq 12 and 13, the following differential equations are obtained:

$$\frac{d\sigma_z}{dr} = \frac{1}{\sigma_z}\left[A \cdot \bar{\sigma} - B \cdot \frac{\bar{\sigma}\left(\ln \frac{r}{r_u}\right)^2}{\left(\frac{\bar{\sigma} - \sigma_s}{k}\right)^{2/n}} + \frac{4(P + R + PR)^2}{nk\left(\frac{\bar{\sigma} - \sigma_s}{k}\right)^{(n+2)/n}} \right] \cdot \frac{d\bar{\sigma}}{dr} - B \cdot \frac{\bar{\sigma}^2 \ln \frac{r}{r_u}}{r\sigma_z \left(\frac{\bar{\sigma} - \sigma_s}{k}\right)^{2/n}} \qquad \text{(Eq 16)}$$

$$\frac{d\sigma_x}{dr} = C \cdot \left[\frac{\ln \frac{r}{r_u}}{\left(\frac{\bar{\sigma} - \sigma_s}{k}\right)^{1/n}} - \frac{\bar{\sigma} \ln \frac{r}{r_u}}{nk\left(\frac{\bar{\sigma} - \sigma_s}{k}\right)^{1 + n/n}} \right] \cdot \frac{d\bar{\sigma}}{dr} + C \cdot \frac{\bar{\sigma}}{r\left(\frac{\bar{\sigma} - \sigma_s}{k}\right)^{1/n}} + \frac{1}{1 + R} \cdot \frac{d\sigma_z}{dr} \qquad \text{(Eq 17)}$$

where:

$$A = \frac{2(1 + R)(P + R + PR)}{3R(1 + P + R)} \qquad B = \frac{4(P + R + PR)^2}{9PR(1 + P + R)}$$

$$C = \frac{2(P + R + PR)}{3P(1 + R)}$$

From Eq 12, 13, 14, 15, 16, and 17, the governing equation that relates the effective stress to the radial position is obtained as:

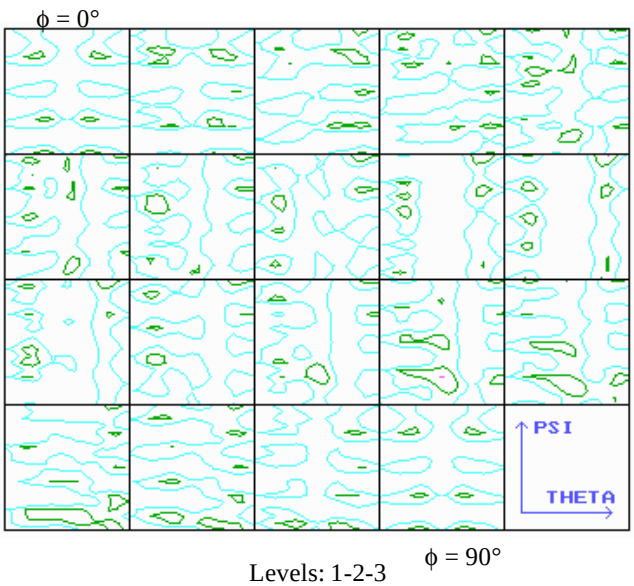

Fig. 3 ϕ sections (Δϕ = 5°) of the ODF of the copper alloy

$$\frac{d\bar{\sigma}}{dr} = \frac{\dfrac{B \cdot \bar{\sigma} \ln \dfrac{r}{r_u}}{r\left(\dfrac{\bar{\sigma} - \sigma_s}{k}\right)^{2/n}}}{A - B \cdot \dfrac{\left(\ln \dfrac{r}{r_u}\right)^2}{\left(\dfrac{\bar{\sigma} - \sigma_s}{k}\right)^{2/n}} + B \cdot \dfrac{\bar{\sigma}\left(\ln \dfrac{r}{r_u}\right)^2}{nk\left(\dfrac{\bar{\sigma} - \sigma_s}{k}\right)^{(2+n)/n}} - D}$$

$$D = \frac{-\left[A \cdot \bar{\sigma}^2 - B \cdot \dfrac{\bar{\sigma} 2\left(\ln \dfrac{r}{r_u}\right)^2}{\left(\dfrac{\bar{\sigma} - \sigma_s}{k}\right)^{2/n}}\right]^{1/2}}{nk\left(\dfrac{\bar{\sigma} - \sigma_s}{k}\right)^{1-(1/n)}} \quad \text{(Eq 18)}$$

When the position of the unstretched fiber and the shape of the cross-sectional geometry are known, the effective stress, $\bar{\sigma}$, the circumferential stress, σ_x, and the radial stress, σ_z, can be found from Eq 18, 12, and 13, respectively. The bending moment per unit length is then obtained by integrating σ_x over the cross section of the strip. Thus:

$$M = \int_{r_i}^{r_y} \sigma_x \, w r dr \quad \text{(Eq 19)}$$

In the model, the springback is assumed to result from purely elastic recovery. Thus:

$$\frac{1}{r'} = \frac{1}{r} - \frac{M}{EI} \quad \text{(Eq 20)}$$

The unstretched fiber is taken as the springback axis so that the lengths of the fibers before and after the springback is equal. Then, the final angle after springback is given by:

$$\theta' = \frac{r_u}{r'_u} \cdot \theta \quad \text{(Eq 21)}$$

where θ is the bending angle.

A computer program has been developed to simulate the bending process. The computation scheme of the program is shown in Fig. 2. In the first step, the strip is bent from 0° to a small increment of angle. After the effective stress of the strip is determined by the Runge-Kutta method, the changed cross-sectional geometry of the strip is also obtained, which provides the necessary information for the next step. The strip is further deformed until the total bending angle equals the predefined angle. Based on the predicted change in final thickness and the bending moment of the strip, the springback angle is easily determined.

3. Results and Discussion

In this article, the deformation behavior and springback of a typical leadframe copper alloy have been investigated. The experimental springback behavior of the copper alloy has been reported by Fu et al. (Ref 1). In order to establish the state of anisotropy and related mechanical properties of the material, its crystallographic texture was measured by a "Philips" x-ray diffractometer. Three incomplete pole figures: (111), (200), and (220) were obtained by the back reflection method at 5° increments using copper Kα radiation. From the pole figures, orientation distribution function (ODF) was calculated using the software developed by Cai and Lee using the series expansion method (Ref 8). Figure 3 shows the measured ODF of the copper alloy. Based on the model developed by Cai and Lee (Ref 8), the anisotropic properties and the stress-strain curve of the material were predicted from the ODF. Figure 4 illustrates the predicted *R* values of the alloy at different angles to the rolling directions. It is shown that the material exhibits a certain degree of anisotropy. The predicted stress-strain curves of the material in the directions parallel and perpendicular to the rolling direction, which are shown in Fig. 5, can be represented by the following empirical equations:

$$\bar{\sigma} = 403.92 + 1971.43\bar{\varepsilon}^{0.59} \text{ (rolling direction)}$$

and

$$\bar{\sigma} = 398.76 + 1828.74\bar{\varepsilon}^{0.59} \text{ (transverse direction)}$$

Using the present anisotropic plane stress model, the deformation behavior and springback of the alloy sheet, using a 90°

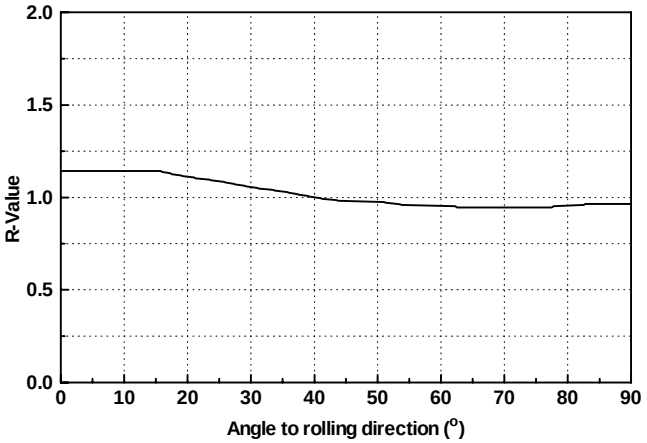

Fig. 4 Variation of *R* values

die and different die radii, have been computed. The step size used in the program is 1°. Figure 6 shows the predicted relationship between die radius and current thickness of the alloy along the rolling direction and the transverse direction. The corresponding relationship for the isotropic plane stress model is superimposed in the graph for comparison. It is found that the strip thickness decreases with decreasing die radius. For a given die radius, the strip thickness predicted by the isotropic model lies between the predictions by the present model. Figure 7 indicates the change in width of a bent strip in the radial direction for die radii equal to 0.30, 0.20, and 0.15 mm. It is found that the width change in the radial direction for a strip having its length in the rolling direction is greater than that when the length is in the transverse direction. The variation of width change along the thickness direction leads to a distorted trapezoidal cross section of the strip. A more distorted cross section is expected for the strip deformed along the rolling direction.

Figures 8(a) and (b) show the radial and circumferential stresses of the alloy strip at a die radius of 0.3 mm. It can be seen from Fig. 8(a) that larger compressive stress is obtained when the strip length is in the rolling direction, whereas, smaller compressive stress is predicted when the strip is perpendicular to the rolling direction. From Fig. 8(b), it is observed that the circumferential stress, which varies with the radial position, is positive when the radial position is above the neutral axis and negative when the radial position is below the neutral axis. It is also expected that larger circumferential and radial stress will result in larger springback angle. Figure 9 shows stress distributions of the strip for all the three die radii. It is observed that the circumferential stress decreases with decreasing die radius

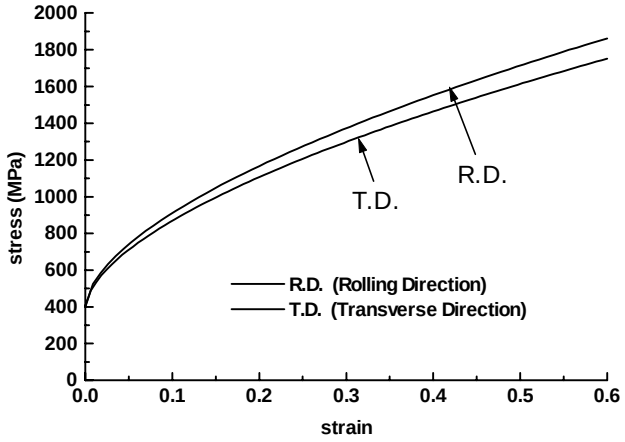

Fig. 5 Predicted stress-strain curve

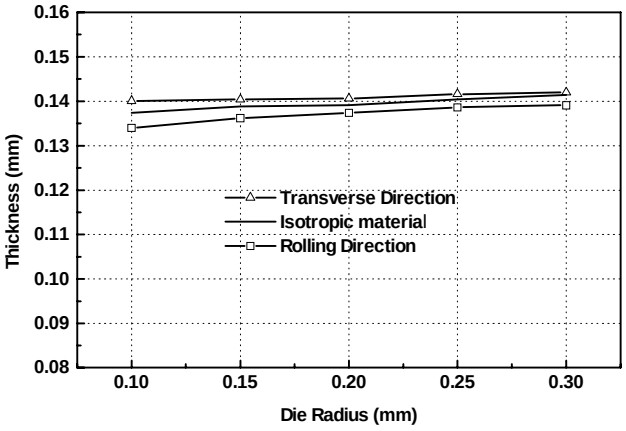

Fig. 6 Relationship between strip thickness and internal bend radius

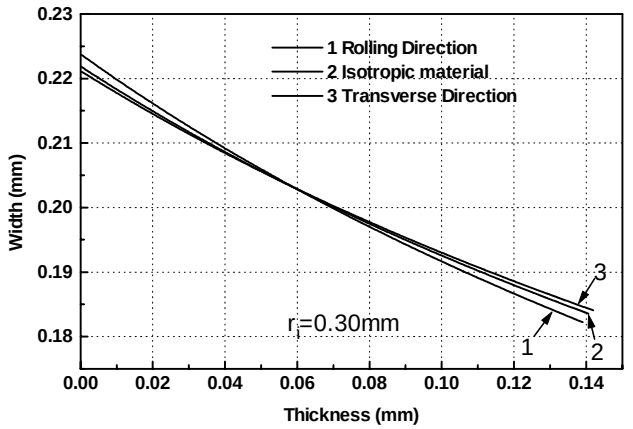

(a)

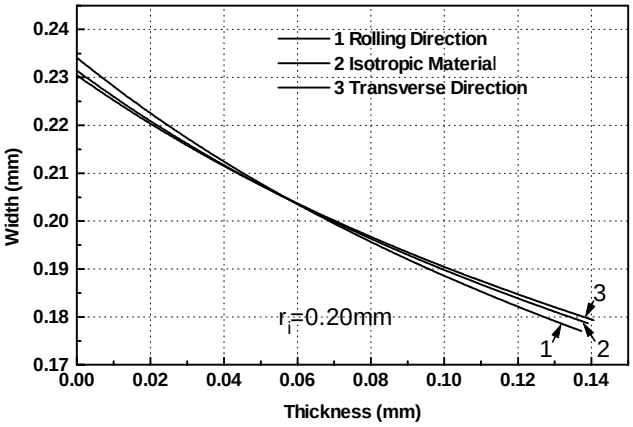

(b)

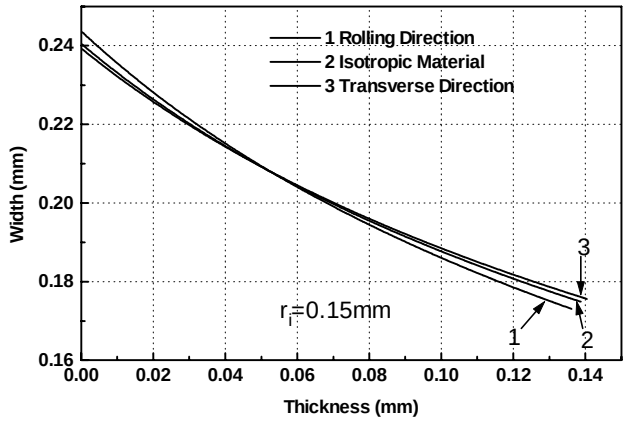

(c)

Fig. 7 Width change along the thickness direction

when the radial position is below the neutral axis and increases with decreasing die radius when the radial position is above the neutral axis. This is because a large die angle or a bending radius result in smaller circumferential stresses and strains.

Figure 10 illustrates the comparison between experimental springback angles of the copper alloy strip and those predicted by the present theoretical model. The experimental results reported by Fu et al. (Ref 1) indicate that the springback angle of the strip, taken along the rolling direction, is larger than that along the transverse direction. It is worth mentioning that the prediction made by the previously proposed isotropic model does not explain the experimental findings. Meanwhile, the new anisotropic model gives a consistent relationship between predicted and experimental results, although a relatively large discrepancy exists between the two. It should be noted that the experimental results were obtained using a roller forming jig developed by Fu et al. (Ref 1). Roller forming is one of the common forming methods for IC packages. The assumption of pure bending in the model may be the major reason for the discrepancy. Of course, there are reasons, such as the change in the state of anisotropy of the alloy during bending. An improvement on the model, taking into consideration friction or other factors observed in roller bending, will be pursued in the future.

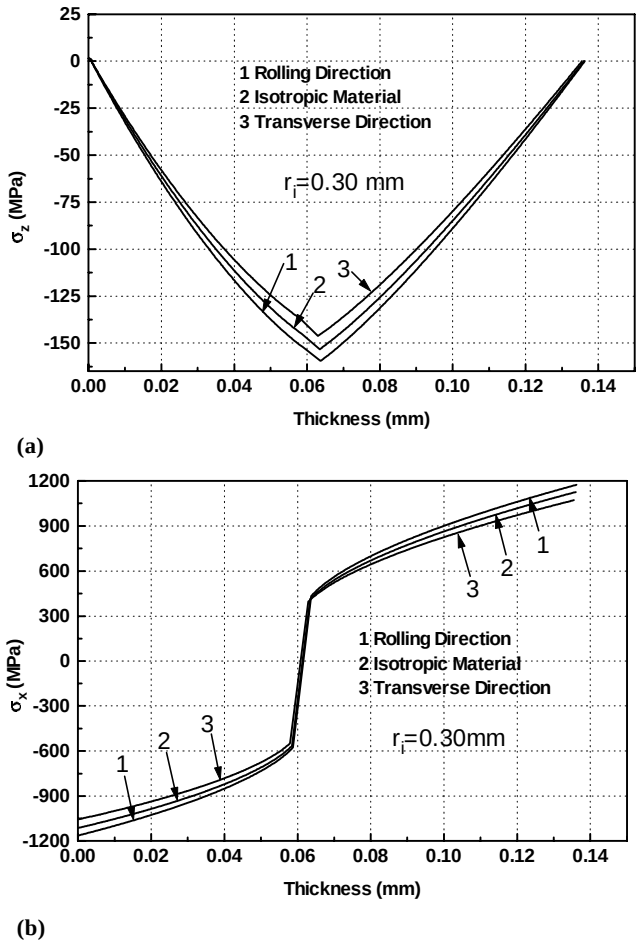

Fig. 8 (a) Radial stress distribution. (b) Circumferential stress distribution

4. Conclusions

In this article, a new plane stress bending model, taking into account plastic anisotropy, has been proposed to predict the deformation behavior and springback of narrow strips. The trend of the predictions made by the anisotropic model is shown to be in agreement with the experimental findings. It is found that the isotropic bending model is unable to explain the springback behavior of the anisotropic leadframe materials. Although much improvement of the model such as the consideration of friction in the bending process has to be completed in order to give a more accurate prediction, the findings of the paper are highly significant in providing useful guidelines for tool designers and in better understanding the springback behavior of anisotropic leadframes.

Acknowledgment

The authors wish to express their gratitude for the financial support of the project rendered from the Hong Kong Research Grant Council, under code No. 354/100.

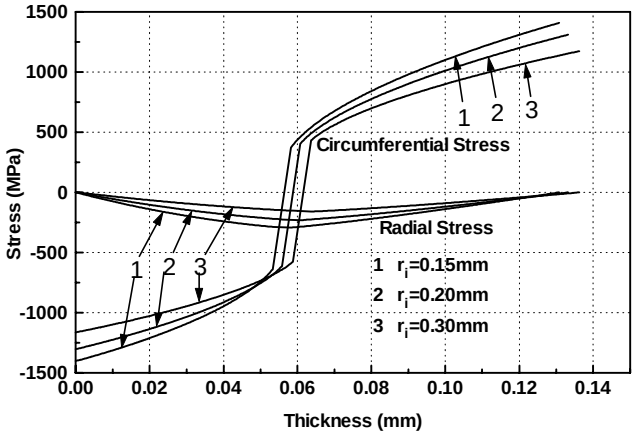

Fig. 9 Stress distribution for bending along the rolling direction

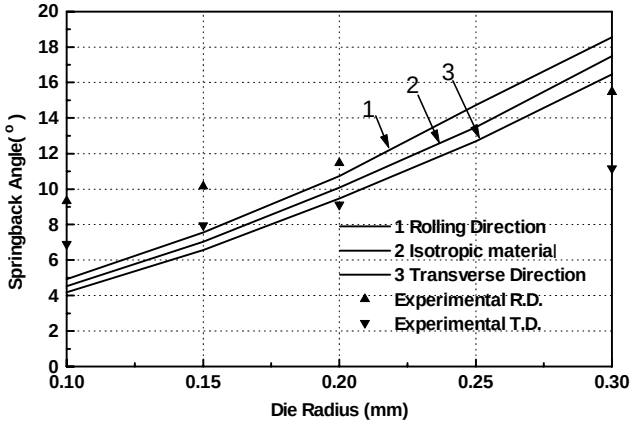

Fig. 10 Comparison between experimental springback angle and the theoretical predictions

References

1. M.H. Fu, K.C. Chan, W.B. Lee, and L.K. Chan, Springback in the Roller Forming of Integrated Circuit Leadframes, *J. Mater. Process. Technol.*, Vol 66, 1997, p 107-111
2. K.C. Chan and S.H. Wang, Theoretical Analysis of Springback in Bending of Integrated Circuit Leadframes, *J. Mater. Process. Technol.*, in print
3. P. Lequeu and J.J. Jonas, Modelling of the Plastic Anisotropy of Textured Sheet, *Metall. Trans. A*, Vol 19, 1988, p 105-120
4. K.C. Chan and W.B. Lee, A Theoretical Prediction of the Strain Path of Sheet Metal Deformed under Uniaxial and Biaxial Stress State, *Int. J. Mech. Sci.*, Vol 32, 1990, p 497-511
5. D.V. Wilson, A.R. Mirshams, and W.T. Roberts, An Experimental Study of the Effect of Sheet Thickness and Grain Size on Limit-Strains in Biaxial Stretching, *Int. J. Mech. Sci.*, Vol 25, 1983, p 859-870
6. D.V. Wilson and P.M.B. Rodrigues, On the Directionality of Strain Localization When Stretching Aluminum Alloy Sheets in Biaxial Tension, *Metall. Trans. A*, Vol 17, 1986, p 367-370
7. R. Hill, The Mathematical Theory of Plasticity, Oxford University Press, 1950
8. M.J. Cai and W.B. Lee, The Development of a Computer Software System for the Prediction of Formability Parameters of Sheet Metals from X-Ray Diffraction Data, *J. Mater. Process. Technol.*, Vol 48, 1995, p 51-57